Clays and Clay Minerals, Vol. 57, No. 3, 311–329, 2009.

THE OCCURRENCE AND ORIGIN OF THE SÖĞÜT KAOLINITE DEPOSITS IN THE PALEOZOIC SARICAKAYA GRANITE-GRANODIORITE COMPLEXES AND OVERLYING NEOGENE SEDIMENTS (BILECIK, NORTHWESTERN TURKEY)

SELAHATTİN KADİR* AND FİRDEVS KART

Eskişehir Osmangazi University, Department of Geological Engineering, TR-26480 Eskişehir, Turkey

Abstract—The Söğüt kaolinite deposits at Çaltı, İnhisar, and Küre, Turkey, are an important source of raw materials for the ceramics industry of that country, but no detailed mineralogical or geochemical characterizations of these economically important materials have been carried out to date. The purpose of this study was to fill this gap by performing mineralogical, geochemical, and isotopic characterizations of these kaolinite deposits which occur within Paleozoic granite-granodiorite complexes that are crosscut by aplite and pegmatite dikes, and overlain by Neogene sedimentary units. These units are dominated by quartz veins and networks of subvertical fractures and weak zones that were invaded by hydrothermal fluids, resulting in their kaolinization and silicification. Altered units and related host rocks were examined using polarized-light microscopy, X-ray diffractometry, scanning electron microscopy, infrared spectroscopy, and chemical and isotopic methods. Feldspar crystals are either sericitized or kaolinized, and mica exhibits partial chloritization; Fe-Ti-Mn oxides occur within fractures. Kaolinite crystals occur in authigenic vermiform or plate-like stacked forms, having contacts with resorbed feldspar crystals which locally exhibit thick, platy, and subparallel orientations relative to microfractures, the pathways for hydrothermal-fluid injection. Altered feldspar relicts are associated mainly with kaolinite, smectite, quartz crystals, and illite/mica. Increase in (Al+Fe)/Si in the kaolinized units (relative to host-rock granite and granodiorite complexes and silicification), depletion of Ba+Rb, and a negative Eu anomaly reveal that the alteration of feldspar by hydrothermal fluid, the character of which was determined from O- and H-isotopic values, resulted in the precipitation of kaolinite. Thus, the Söğüt kaolinite deposit possibly formed by hydrothermal alteration and a feldspar dissolution-precipitation mechanism in both the granite-granodiorites complexes and related overlying sedimentary units under acidic environmental conditions, which developed *via* depletion of the soluble elements Na and Ca.

Key Words—Geochemistry, Granite-granodiorite Complexes, Hydrothermal Alteration, Kaolinite, Mineralogy, Sedimentary Units, Stable Isotopes, Turkey.

INTRODUCTION

Kaolinite deposits in granitic rocks develop either by hydrothermal, weathering, or mixed hydrothermal-weathering processes (Exley, 1976; Bristow, 1977; Kitagawa and Köster, 1991). The chemical alteration of feldspar, mica, and chlorite by hydrothermal fluids or meteoric water results in the precipitation of kaolinite (Gilkes and Suddhiprakarn, 1979a, 1979b; Harris *et al*., 1985a, 1985b; Rebertus *et al*., 1986). The varying mobilities of major and trace elements during the alteration of precursor minerals, such as feldspar ± mica, may result in the concentration of Al ± Fe and the leaching of alkali elements, favoring precipitation of kaolinite in an acidic environment (Zielinski, 1985; Gouveia *et al.*, 1993; Garbarino *et al.*, 1994; Ekosse, 2001; Maiza *et al.*, 2003; Njoya *et al.*, 2006; Siddique and Ahmet, 2008; Gürel and Kadir, 2008). Under well drained, warm, and humid conditions, mica is transformed to kaolinite following intermediate stages characterized by hydrobiotite, vermiculite, smectite, or even by direct transformation of mica to kaolinite (Stock and Sikora, 1976; Rebertus *et al.*, 1986; Kadir and Akbulut, 2009).

The Söğüt kaolinite deposits, hosted by granite-granodiorite complexes and related overlying sedimentary units, are collectively one of the most important raw-material sources for ceramic companies in Turkey, with 500,000 tons of (inferred) minable reserves and 1,000,000 tons of inferred + probable reserves (8th Five-Year Development Plan – State Planning Organization of Turkey, 2001). Pegmatitic deposits at Çaltı, İnhisar, and Küre are mined for kaolinite. The white and reddish kaolinite zones developed along silicified and mainly sub-vertical Fe oxide-bearing fractures and veins within strongly altered granitic and granodioritic units. The origin of kaolinite in the granite-granodiorite complexes and overlying sedimentary units is open to debate.

The kaolinite-rich Söğüt region of Turkey has been studied for its general geology, economic geology (Akıncı, 1968; Kalyoncuoğlu *et al.*, 1977; Aksoy, 1978), and sedimentology, lithofacies and mineralogy (Gençoğlu, 1988; Gençoğlu *et al.*, 1989; 1:100,000 scale

* E-mail address of corresponding author:
skadir_esogu@yahoo.com
DOI: 10.1346/CCMN.2009.0570304

Geological Map of Turkey, Duru *et al.*, 2002). No detailed mineralogical or geochemical characterizations of these economically important kaolinite deposits have been carried out to date. The purpose of this study was to characterize the mineralogical, geochemical, and isotopic properties of these kaolinite deposits, and to discuss their mode of origin within the Paleozoic granitic and granodioritic complexes, which are crosscut by aplite and pegmatite dikes and overlain by Neogene sedimentary units.

METHODS

Samples were collected from the Söğüt area in order to identify the lateral and vertical distribution of kaolinite within the granite-granodiorite-pegmatite-aplite complexes and overlying sedimentary units (Figures 1, 2).

In all, 65 samples representing the various facies were analyzed for their mineralogical characteristics by polarized-light microscopy (Leitz Laborlux 11 Pol), X-ray powder diffractometry (XRD) (Rigaku-Geigerflex), and scanning electron microscopy (SEM-EDX) (JEOL JSM 84A-EDX). The XRD analyses were performed using CuKα radiation at a scanning speed of 1º2θ/min. Random powders of whole-rock samples were used to determine the bulk mineralogy. The clay mineralogy was determined *via* separation of the clay fraction (<2 μm) by sedimentation, followed by centrifugation of the suspension after overnight dispersion in distilled water. The clay particles were dispersed by ultrasonic vibration for ~15 min. Oriented specimens of the <2 μm fraction were prepared from each sample (air dried, then ethylene glycol solvated at 60ºC for 2 h, and thermally treated at 350ºC and 550ºC for 2 h). Semi-quantitative relative abundances of rock-forming minerals were established according to the method of Brindley (1980), whereas the relative abundances of minerals in the clay-mineral fractions were determined using their basal reflections and the intensity factors of Moore and Reynolds (1989). The presence of opaque minerals was determined by reflected-light microscopy (Leitz MPV-SP). Representative clay-dominated bulk samples were prepared for SEM-EDX analysis by adhering the fresh, broken surface of each rock sample onto an aluminum sample holder with double-sided tape, and then coating with a thin film of gold (350 Å) using a Giko ion coater.

Chemical analyses of 23 fresh and altered whole-rock samples were carried out at Acme Analytical Laboratories Ltd. (Canada) using inductively coupled plasma-atomic emission spectroscopy for major and trace elements and inductively coupled plasma-mass spectrometry for rare-earth elements (*REE*). The detection limits for the analyses were between 0.01 and 0.1 wt.% for major elements, between 0.1 and 5 ppm for trace elements, and between 0.01 and 0.5 ppm for *REE*.

Elemental enrichments and depletions were estimated using the procedure of MacLean and Kranidiotis (1987). In these calculations, Zr was assumed to be the most immobile element, based on calculated correlation coefficients with other elements. All samples were grouped on the basis of degree of alteration (average result from each group), and the gains and losses of components were calculated using a starting mass of 100 g of average fresh anhydrous sample. The equation used in these calculations can be written for SiO_2 (MacLean and Kranidiotis, 1987) as:

$$SiO_2 = \frac{SiO_2 \text{ wt.\% altered rock}}{\text{Zr ppm altered rock}} \times \text{Zr ppm fresh rock}$$

Mass gains and losses were determined by subtracting the calculated values from the concentrations of components in the least-altered samples using the formula above.

Three kaolinite samples were analyzed for stable isotopes of H and O by the Marmara Research Center Laboratory (Kocaeli) of the Scientific and Technological Research Council of Turkey (TUBİTAK) using EA-GC/IRMS model equipment. The H- and O-isotopic analyses were reported in the standard delta notation as per mil deviations from V-SMOW. Stable isotopes were determined on the <2 μm fractions for samples A6, B3, and E2 (*i.e.* those with the greatest kaolinite contents), obtained by sedimentation, followed by centrifugation of the suspension after soaking overnight in distilled water.

GEOLOGICAL SETTING

The basement of the study area consists of pre-Miocene metamorphic and igneous rocks (Demirkol, 1977) (Figures 1, 2). Metamorphic basement rocks, as well as the Sarıcakaya granite and granodiorite complexes, are crosscut by aplite and pegmatite dikes and quartz veins in the Söğüt area, which occupy mainly subvertical fractures and a network of cracks (Demirkol, 1977; Göncüoğlu *et al.*, 2000). The pegmatite dikes are coarsely crystalline, generally 1 m wide, and dominated by orthoclase and microcline; the aplite dikes are 40 cm wide. The contacts of these dikes with granitic-granodioritic rocks exhibit cataclastic texture, accompanied by abundant kaolinization and silicification, and filling by Fe oxides; these rocks are also friable. The friable material is white, cream-colored, or light brown and stains the hand when touched; siliceous material exhibits toughness. The granites are gray and range from coarsely to finely crystalline. Coarsely crystalline granites are intertwined with granodiorite and, together with aplite and pegmatite, cut older granite (Göncüoğlu *et al.*, 1996). These units are of subalkaline character (Kibici, 1982) and bear relicts of basement metamorphic and volcanic rocks. The contact areas of the granite-granodiorite intrusions with greenschist- and amphibolite-facies basement rocks are oriented and contain perthite, biotite, and accessory garnet.

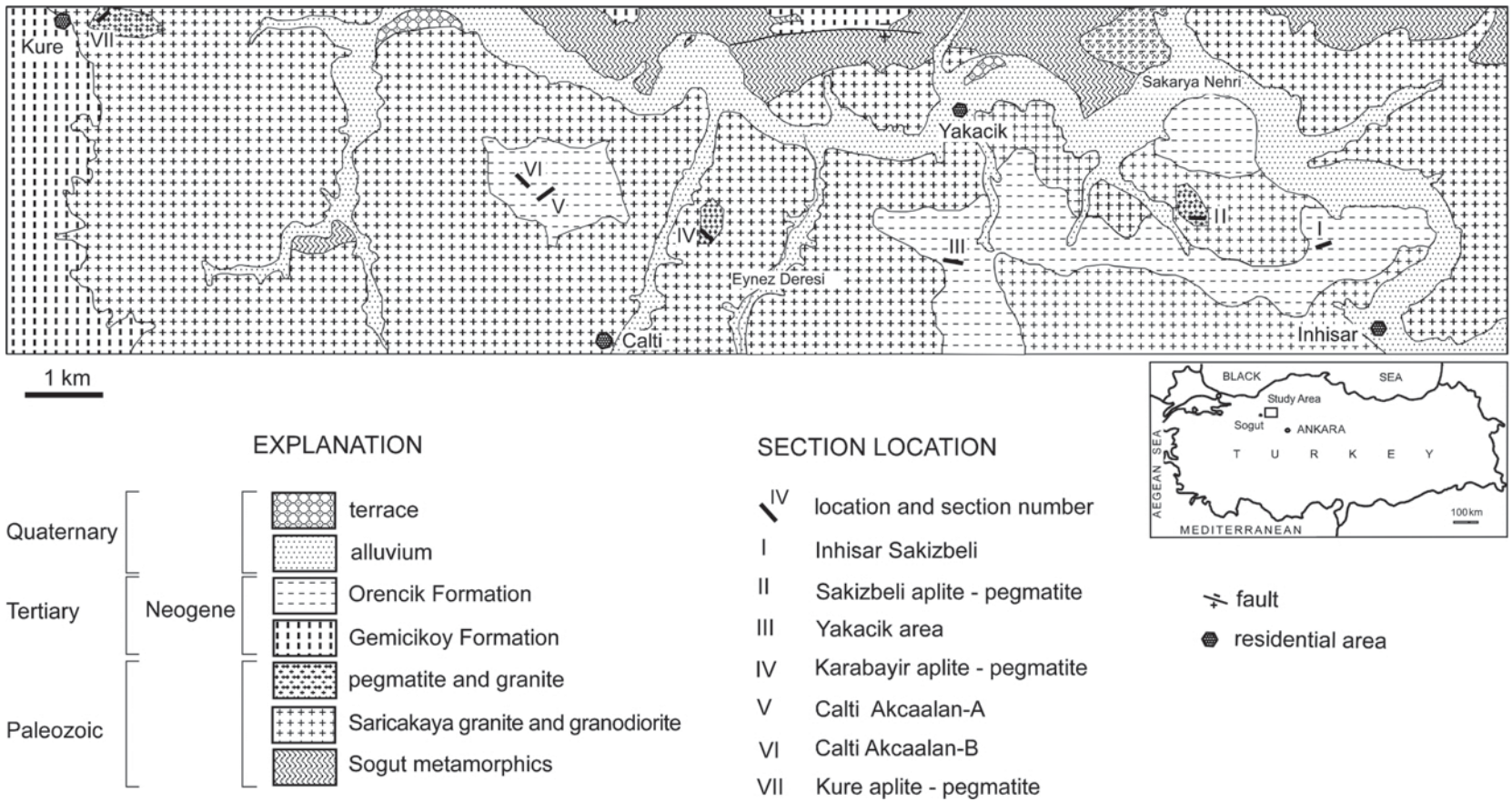

Figure 1. Geological map of the Söğüt kaolinite deposit area (modified from Duru *et al*. (2002) and Kalyoncuoğlu *et al*. (1977)).

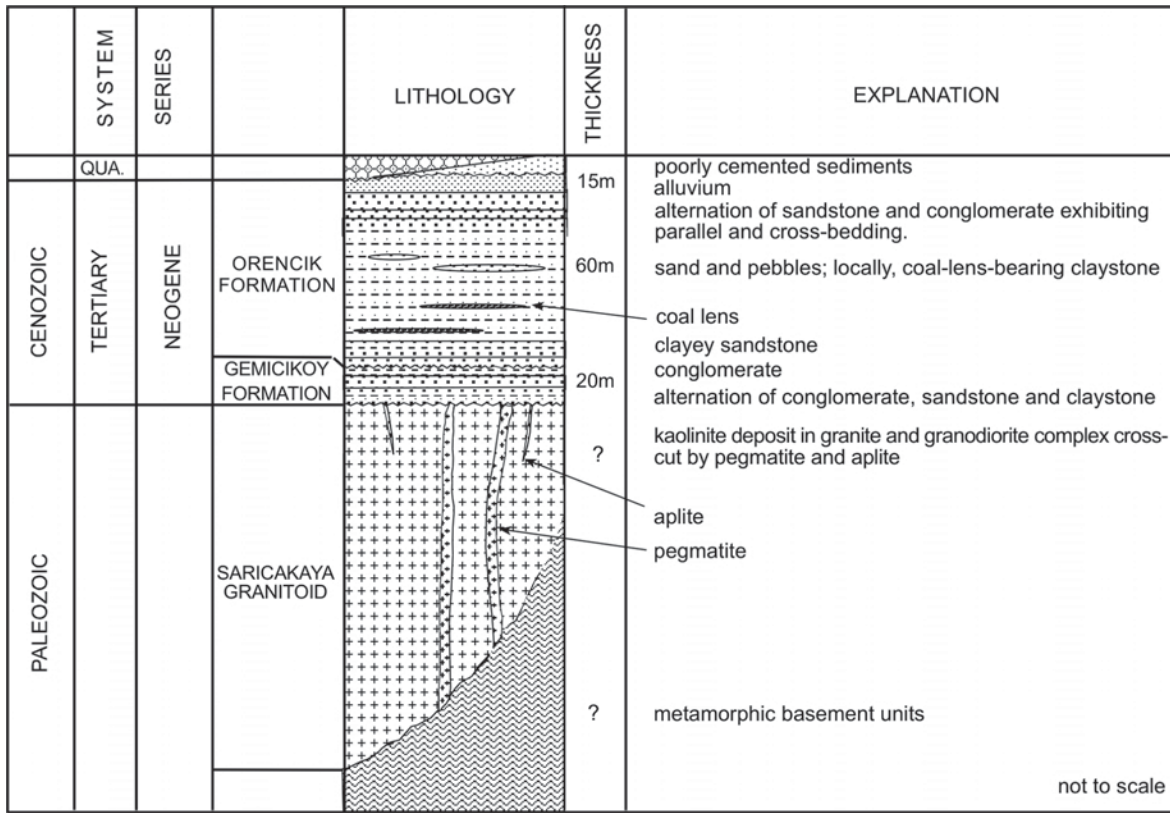

Figure 2. Simplified general stratigraphic section of the study area (modified from Duru *et al.* (2002) and Kalyoncuoglu *et al.* (1977)).

Radiometric age dating of these units yielded ages of 290 m.y. (Çoğulu *et al.*, 1965) and 213–248 m.y. (Delaloye and Bingöl, 2000), or early Permian.

Neogene lacustrine and fluvial sediments consist of alternating red to brownish fluvial and lacustrine conglomerate, sandstone, mudstone, and limestone units which were derived from metamorphic, granitic, granodioritic, aplitic, and pegmatitic rocks (Duru *et al.*, 2002). The lower levels of these sedimentary materials consist, therefore, of weakly to moderately cemented schist, granite, and aplite pebbles, followed upward by clayey, sandy, and coal-bearing levels, intercalated with plastic, clayey layers bearing desiccation cracks, organic matter, root imprints, and leaf fossils, and characterized by conchoidal fracture. These units are followed upward by Quaternary alluvium.

The granitic-granodioritic complexes and overlying sedimentary units of the study area are also under the tectonic influence of the North Anatolian Fault Zone (Şengör, 1979; Şengör and Yılmaz, 1981).

RESULTS

Petrographic determinations

Samples of partially altered aplitic, pegmatitic, granitic, and granodioritic rocks are composed of K-feldspar (orthoclase-microcline), plagioclase (albite-oligoclase), biotite, and quartz (Figure 3). Different degrees of thin-section-scale alteration, such as kaolinization, sericitization, chloritization, and crystallization of Fe-Ti-oxide minerals, have been observed in these units. Feldspar crystals are sericitized and kaolinized, and mica and hornblende are generally converted to chlorite, and relatively dark colors characterize the biotite and hornblende due to the oxidation of iron to Fe^{3+}, present as oxybiotite and oxyhornblende, with corroded, xenomorphic crystal shapes especially in highly fractured zones (Figure 3a–e). With intensifying alteration toward the microfractures, kaolinite + illite/mica ± Fe oxide ± chlorite + silica dominate; thus, the primary minerals are converted to clay minerals and Fe-Ti-oxides. Relict feldspar crystals and their alteration products are generally associated with quartz crystals. Fe oxides occur in microfractures and within weak zones of the granite-granodiorite and overlying sedimentary units (Figure 3d–e). On the other hand, in the clayey sedimentary units, altered feldspar, quartz, and clay particles exhibit subparallel sedimentary (bedding) features (Figure 3e–f). These sediments consist of quartz, highly altered feldspar, and oxybiotite grains cemented by clayey materials.

Goethite and lepidocrocite are dominant in most of the silicified and altered samples as determined *via* reflected-light microscopy. These materials also enclose

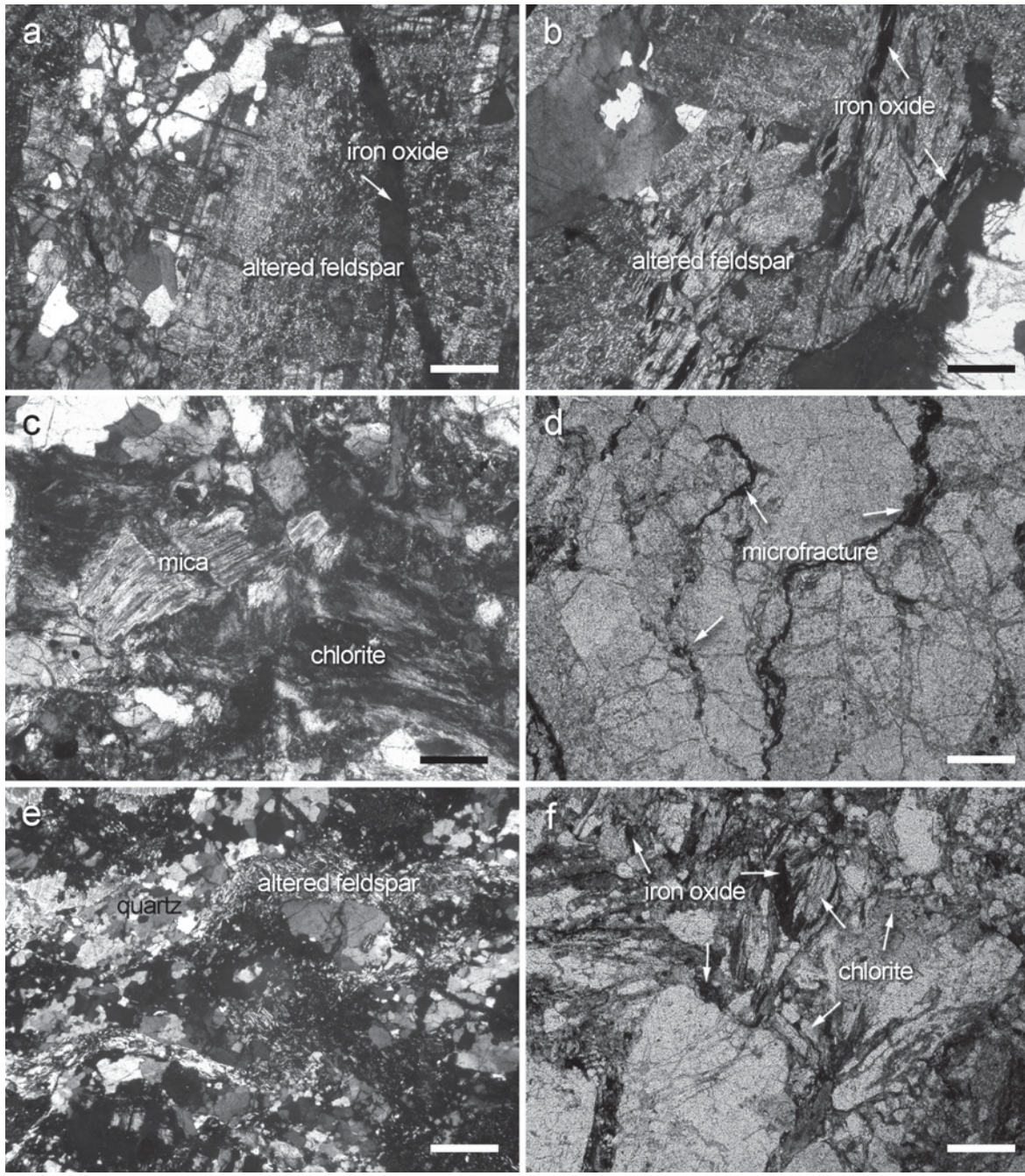

Figure 3. Photomicrographs showing: (a–b) the relationship between a sericitized and kaolinized feldspar crystal with an Fe oxide-filled microfracture, in a sample from the granite-granodiorite unit (crossed polars (A-1), scale bar = 0.25 mm); (c) altered mica rimmed by chlorite and Fe oxide (crossed polars (J-4)); (d) highly fractured and resorbed granite-granodiorite units with evidence of alteration (plane-polarized light (E-2)); (e) development of clayey material as cement between feldspar, quartz, and mica in sedimentary material (crossed polars (F-1)); (f) clay and Fe oxide as a cement between feldspar, quartz, and mica particles in sedimentary material (plane-polarized light (F-1)).

euhedral to subhedral, acicular to columnar rutile crystals and, locally, scarce yellowish-white pyrite relics or dark-gray manganite coexisting mainly with goethite.

XRD determinations

Kaolinite, smectite, illite, and chlorite are the main alteration products associated with K-feldspar, plagio-

Table 1. Mineralogical variation through the stratigraphic sections of the Söğüt area.

Sample	Rock type	kao	smc	chl	ill/mc	fds	qtz	gt	dol	cal
A-1	Granite-granodiorite	+	+			+	+		acc	
A-2	Granite-granodiorite	+	++			+	+			
A-3	Granite-granodiorite	++	++		acc	+	+			acc
A-6	Granite-granodiorite	+++	acc		acc	+	+			
A-8	Granite-granodiorite	++	acc			+	+		acc	
B-2	Granite-granodiorite	+++	+		acc	+	+			acc
B-3	Granite-granodiorite	++++	acc		acc	acc	acc			
B-4	Granite-granodiorite	++	++			acc	+		+	acc
E-2	Granite-granodiorite	+++	+		acc	+	+	acc		
E-4	Granite-granodiorite	+	acc		+	+	+			
E-5	Granite-granodiorite	++			++	+	+			
E-6	Granite-granodiorite	+			+	+	+			
E-7	Granite-granodiorite	++	acc		+	+	+	acc		
E-10	Granite-granodiorite	++	ac		acc	+	+			
J-4	Granite-granodiorite	+	+		acc		+	+		
J-5	Granite-granodiorite	++	acc		acc	acc	+			
J-6	Granite-granodiorite	++	+		acc	+	+			
J-9	Granite-granodiorite	+	acc		+	+	+			
C-2	Claystone	+	acc		acc	acc	++			
C-3	Clayey conglomerate	++		acc	+	acc				
C-4	Claystone	++	acc		+	acc	+	acc ?		
C-6	Clayey siltstone	++		acc	++	acc	+			
C-8	Laminated claystone	++		+	++	acc	+			
C-9	Claystone	++	acc		+	acc	+			
D-7	Coal-bearing claystone	++	+		+	acc	+			
D-8	Coal-bearing claystone	++	acc		acc	+	++			
D-12	Claystone	++	+		+	acc	+			
D-14	Claystone	++	+	+	+	+	+			
D-19	Clayey siltstone	+	+	acc		acc		+	+	
D-20	Altered granite	++			acc	+	++		acc	acc
F-3	Sandy conglomerate	+	+		acc	acc	+		acc	acc
F-4	Granite-granodiorite	+	acc		acc	acc	+			
F-5	Claystone	+	acc		acc	acc	+			
F-9	Claystone	++	acc		+	acc	+			
F-10	Coal with claystone	++	acc		+	acc	+			
F-13	Claystone	+			+	acc	+			
K-2	Claystone	+			+	acc	++			
K-3	Mudstone	+			acc	acc	++			
K-8	Mudstone	+	+		+	+	+	acc		
K-9	Claystone	++	acc		acc	acc	++			
K-10	Silty sandstone	++	acc		+	acc	++			

kao: kaolinite, smc: smectite, chl: chlorite, ill/mc: illite/mica, fds: feldspar, qtz: quartz, gt: goethite, dol: dolomite, cal: calcite, +: relative abundance of mineral, acc: accessory.
A–B: Küre, C–D–E: Çatlı, F–J: İnhisar, K: Yakacık.

clase, and quartz, and locally goethite, dolomite, and calcite (Table 1). In the rocks of the granitic-granodioritic complexes, kaolinite is prevalent, accompanied by feldspar, quartz, and illite. A sub-inverse relationship was observed between feldspar and illite. Although the volume percentage of quartz is generally consistent in the pegmatitic units, it occurs in greater concentrations in the upper sedimentary levels. In general, a close relationship between kaolinite and smectite, and the occurrence of goethite, is apparent.

The kaolinite is characterized by very sharp, intense reflections at 7.14 and 3.57 Å, and well defined, non-basal reflections indicate well ordered kaolinite rather than disordered kaolinite and halloysite (MacEwan and Wilson, 1980; Wilson, 1987) (Figure 4). The basal reflection of kaolinite at 7.14 Å is not affected by

ethylene-glycol treatment, but the intensity of this peak decreased at 350ºC and collapsed when heated to 550ºC. At 14.8 Å, the peak is diagnostic of smectite, which expanded to 16.98–17.13 Å following ethylene-glycol solvation and collapsed to 10 Å upon heating to 350ºC; additional heating to 550ºC caused further reduction in

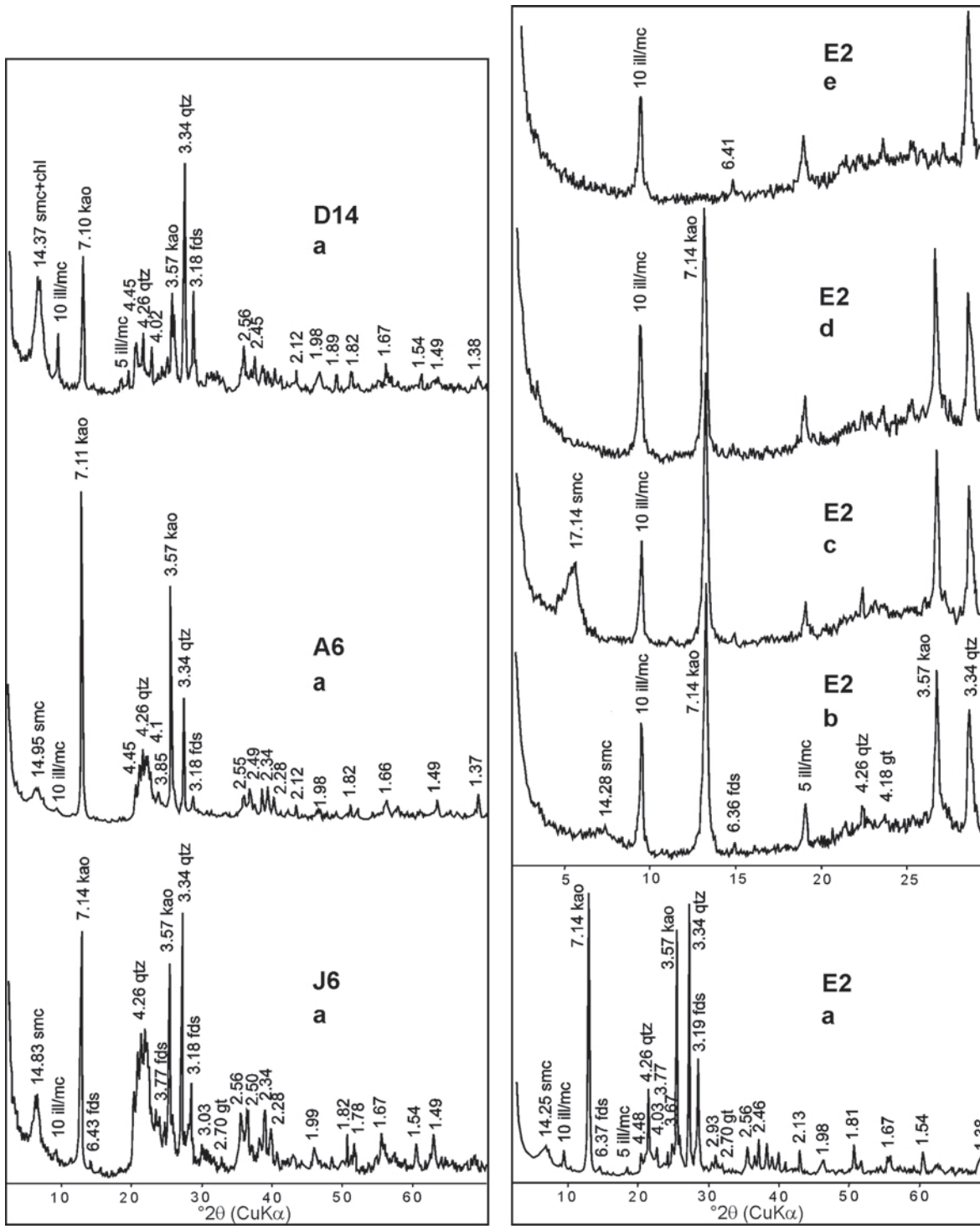

Figure 4. XRD patterns for bulk clayey materials and clay-mineral fractions of samples D14, A6, J6, and E2 from the Söğüt area: (a) powder; (b) oriented; (c) ethylene-glycol solvated; (d) heated to 350ºC; (e) heated to 550ºC. kao: kaolinite, smc: smectite, chl: chlorite, ill/mc: illite/mica, fds: feldspar, qtz: quartz, gt: goethite.

sharpness and reflection of the peaks (Figure 4). The d_{060} reflection at 1.49 Å may indicate the occurrence of dioctahedral smectite (Moore and Reynolds, 1989). Chlorite is identified by a peak at 14.15 Å which is unaffected by ethylene-glycol treatment and by heating to 350ºC and 550ºC. Illite is determined by peaks at 10.0 and 5.0 Å, goethite by peaks at 2.70 and 4.18 Å, plagioclase by a 3.18 Å peak, and K-feldspar by a 3.25 Å peak. The XRD background of some of the kaolinite-bearing samples is slightly elevated, possibly due to the presence of a poorly crystalline phase.

SEM-EDX

Feldspar crystals are highly resorbed and edged mostly by kaolinite plates and stacked plates (Figure 5a–b). Furthermore, some of these kaolinite stacks developed parallel to microfractures, which were possible micro-pathways for hydrothermal fluids (Figure 5c). These fluids also produced alteration of feldspar in the granite-granodiorite complexes and the formation of clayey material among relict materials of the unit. Generally speaking, feldspar crystals that have

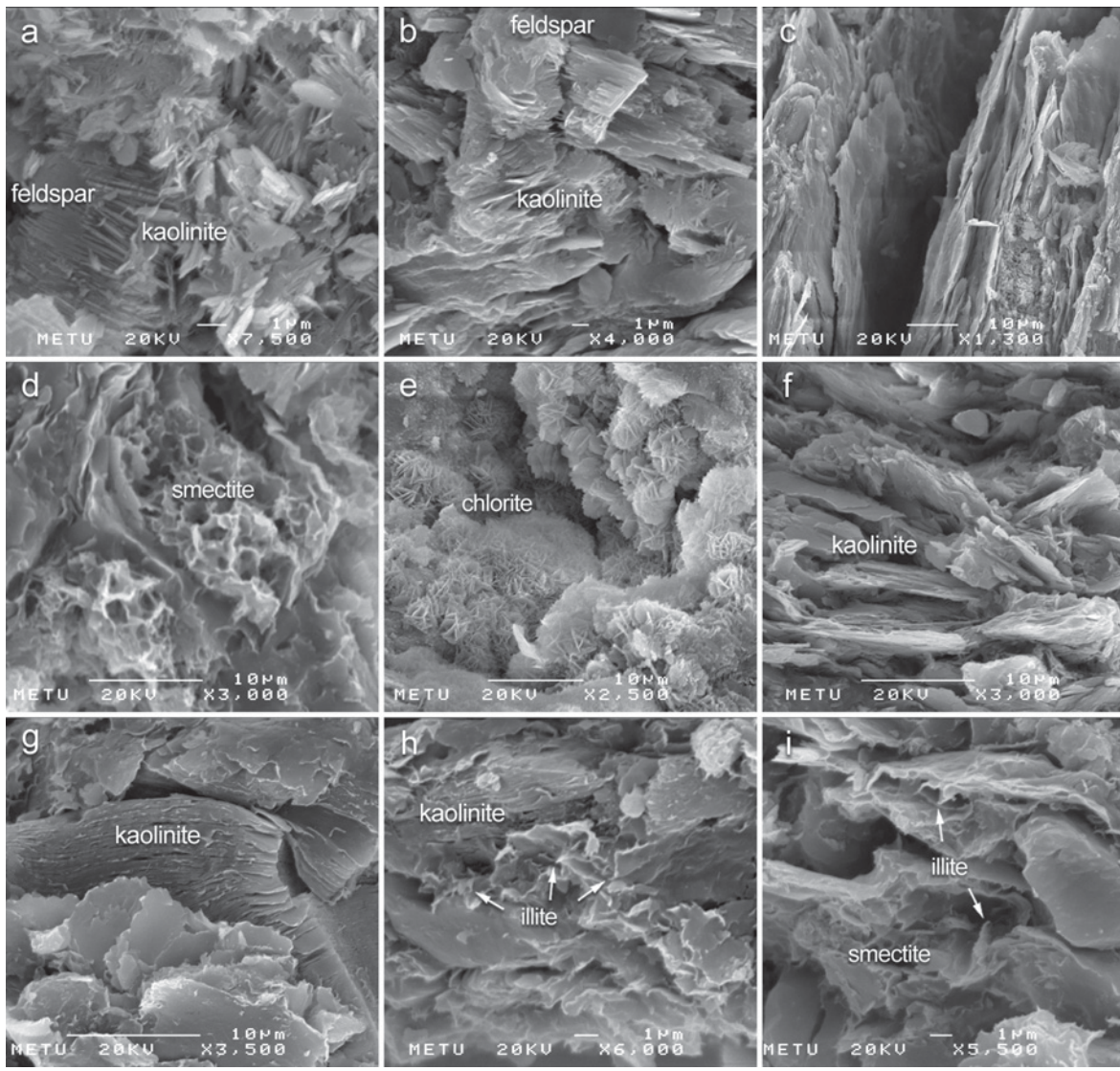

Figure 5. SEM images showing: (a–b) regular growth of authigenic kaolinite plates rimming resorbed feldspar crystals (B-3, J-6); (c) development of oriented, irregular kaolinite stacks situated subparallel to hydrothermal micropathways in a sample from the granite-granodiorite unit (J-6); (d) authigenic growth of cornflake-like smectite in dissolution voids (B-4); (e) authigenic growth of rosette-like chlorite in dissolution voids and on degraded crystals (B-3); (f) irregular kaolinite plates and illite fibers in a sedimentary-unit sample (C-8); (g) accordion- or book-like kaolinite developed authigenically from resorbed feldspar crystals (see Figure 5a)(D-14); (h) the association of platy kaolinite stacks with fibrous illite in a sedimentary-unit sample (D-14); and (i) close-up view of illite and smectite-illite between sedimentary grains (D-14).

been converted to kaolinite consist of individual kaolinite books arranged face-to-face into elongated stacks; intercalated smectite crystals exhibit a well-defined, web-like morphology, which developed as a pore filler and as ribbon-like pore bridges (Figure 5d). Chlorite plates are arranged in rosette patterns and developed within dissolution voids (Figure 5e); these plates are ~2–3 μm in diameter and <1 μm thick. Kaolinite in the sedimentary units exhibits either authigenic, irregular, plate-like stacked forms, or vermiform character coexisting with fibrous illite and relict feldspar (Figure 5f–h). Flaky smectite-illite crystals occur as cement among altered feldspar and quartz crystals (Figure 5i). Individual kaolinite crystals range in diameter from 1 to 10 μm. The diameters of book-like or vermiform kaolinite are greater than those of individual kaolinite crystals.

The EDX analyses indicate that the resorbed feldspar grains consist of albite (Si, Al, Na) and K-feldspar (Si, Al, K). The EDX analysis of the platy structures reveals that these consist of Si and Al, or of Al, Si, Fe, K, and Ti, confirmed to be kaolinite and Fe- + Ti-bearing kaolinite and illite.

IR spectra

The IR spectrum for representative kaolinite sample E-10 (Figure 6) contained sharp bands at 3695, 3652, and 3620 cm^{-1}, characteristic of well-ordered kaolinite (Bobos *et al.*, 2001; Njoya *et al.*, 2006). These bands are assigned to the Al-OH-Al stretching vibration of kaolinite (Farmer and Palmieri, 1975; Van der Marel and Beutelspacher, 1976).

The 1639 cm^{-1} band is related to the deformation vibration of adsorbed minor water coordinated to octahedral Al ± Fe (Van der Marel and Beutelspacher, 1976).

The 1091, 1032, 1004, 696, 648, and 471 cm^{-1} bands are due to the Si-O stretching vibration, and sharp absorption bands at 913 and 937 cm^{-1} are related to the Al-OH-Al of well ordered kaolinite (Bobos *et al.*, 2001; Madejová *et al.*, 1992; Njoya *et al.*, 2006). The subequal lengths of the sharp bands at 797 and 757 cm^{-1} are possibly related to Fe-OH and Al-OH-Si, representative of ordered kaolinite rather than disordered kaolinite where the intensity of the 797 cm^{-1} band is significantly reduced (Russell, 1987; Madejová *et al.*, 1992; Srasra *et al.*, 1994; Njoya *et al.*, 2006). The adsorption bands at 696 and 797 cm^{-1} may also indicate the presence of quartz in the sample. The bands at 539 and 431 cm^{-1} are assigned to Al-O-Si and Si-O-Si, which are related to well-ordered kaolinite (Bobos *et al.*, 2001).

Whole-rock chemical analysis

Whole-rock chemical analyses (Table 2) of samples of the aplite- and pegmatite-bearing granite-granodiorite host rocks (and their alteration products) and overlying clayey sedimentary materials from the kaolinite deposits of the Küre, Çaltı, İnhisar, and Yakacık areas indicated that the major- and trace-element compositions of the samples vary, of course, with mineralogical composition. Large SiO_2 contents (average 74.2%) are accompanied by small quantities of Al_2O_3 (average 14.74%), Fe_2O_3 (average 1.18%), TiO_2 (average 0.39%), and K_2O (average 3.24%) and a small LOI (average 3.80%) in fresh samples. The SiO_2 and K_2O contents of the kaolinized material are smaller (average 58.20%, and 1.63%, respectively) and Al_2O_3 (average 17.89%), Fe_2O_3 (average 5.40%), TiO_2 (average 0.96%), and LOI (10.83%) values are greater. Thus, SiO_2 decreases, but Al_2O_3, Fe_2O_3, TiO_2, and LOI increase with increasing alteration. On the other hand, although the LOI of the kaolinite, which dominates the sedimentary units, is similar to that of the altered granite and granodiorite, the SiO_2 content is smaller (average 54.07%) and Al_2O_3 (average 21.01%), Fe_2O_3 (average

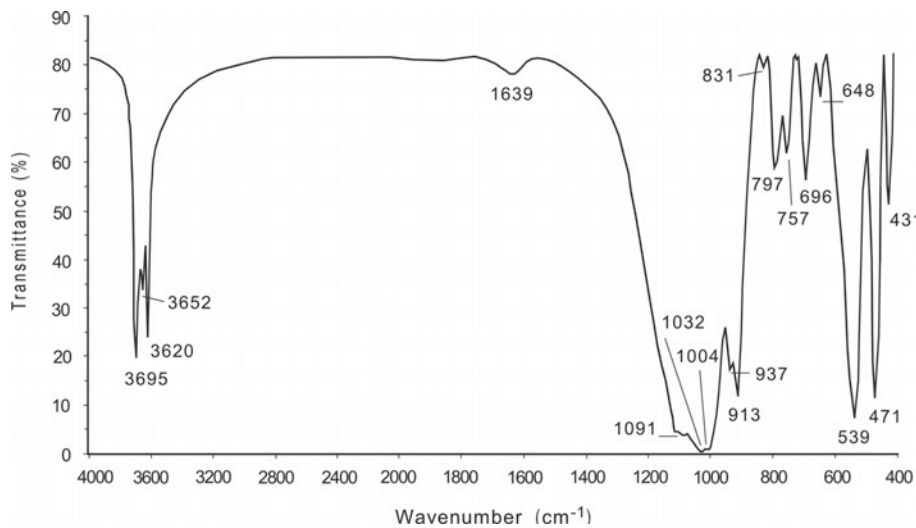

Figure 6. IR spectrum for a Soğüt kaolinite sample (E-10).

5.43%), K_2O (average 2.60%), and TiO_2 (average 1.58%) values are greater.

The mobility of elements plays an important role in the development of the physicochemical environmental conditions necessary for the formation of clay minerals. Thus, mass gains and losses (MacLean and Kranidiotis, 1987) and major- and trace-element enrichments and depletions from fresh (A-1, A-4, A-6, B-2, D-20, E-2, E-6, F-1, J-8, and J-9) to altered samples are observable (Table 3, Figure 7).

K (with related Rb and Ba) and Na were depleted during alteration of K-feldspar and biotite in the granite-granodiorite complexes, except in samples J-9, K-2, and K-8. The degree of depletion of all of these elements is, therefore, positively correlated with kaolinization in both altered granite-granodiorite and overlying sedimentary units. In contrast, Ca (with related Sr) is enriched with advancing kaolinization in both granite-granodiorite and overlying sedimentary units, except in sample J-6. The elevated Al contents reflect the presence of feldspar, illite/mica, kaolinite, and smectite. The Si contents of the whole-rock samples reflect the presence of quartz and feldspar which mainly coexist with kaolinite and, locally, with smectite and illite. The major-oxide elements show that kaolinization was, therefore, negatively correlated with SiO_2 and positively correlated with Al_2O_3-Fe_2O_3-TiO_2 and LOI. Moreover, $SiO_2/Al_2O_3+ Fe_2O_3$ decreases in the kaolinized units in comparison to the granitic, granodioritic, aplitic, and pegmatitic host rocks. Fe_2O_3 and TiO_2 contents in the clay-size fractions increased compared to the fresh granitic, granodioritic, aplitic, and pegmatitic host-rock samples considered to be relatively immobile during alteration. Thus, as detected *via* reflected-light microscopy of selected samples, Fe_2O_3 appears to be bound in Fe-bearing phases such as goethite and lepidocrocite, in sulfide phases such as pyrite, and in Ti-oxide phases such as rutile. Also, on the basis of microchemical analyses carried out by EDX, Fe and Ti occur in the octahedral and interlayer sites of kaolinite, illite, chlorite, and smectite, with Fe possibly substituting for Al, and Ti replacing Fe during physicochemical alteration processes.

Accessory K_2O is related to illite/micas and K-feldspar, while Mg and Ca are situated in dolomite and calcite. MgO and CaO increased with advancing alteration. MgO is related to the presence of chlorite and smectite. CaO is present in calcite and dolomite and, to a lesser extent, in the interlayer site of smectite.

Co, Ni (positively correlated with Fe_2O_3), Cu, Pb, Zn (except in sample J-6), As, Be Y, and V are relatively high in the kaolinized granitic-granodioritic and sedimentary rocks. The distributions of the *REE* are affected by alteration of the granite-granodiorite units and clayey sedimentary units (Tables 2, 3). Light *REE*s (*LREE*) such as La, Ce, and Nd are enriched (with increasing intensity of alteration of the granodiorite) relative to the heavy *REE*s (*HREE*) and kaolinite-bearing sedimentary units, with a negative Eu anomaly in the kaolinized materials, probably reflecting crystal fractionation of plagioclase during alteration of parent materials (Figure 8). Generally, the similar overall *REE* patterns and negative Eu anomalies suggest that kaolinite and coexisting clay-mineral fractions developed by alteration of granitic-granodioritic units and related overlying sediments. Yttrium, Zr, and Nb appear to have been immobile during alteration.

Stable-isotope geochemistry of kaolinite

The O- and H-isotopic compositions of kaolinite-fraction (A6, B3, and E2) samples (Table 4; Figure 9) reveal that the $\delta^{18}O$ values range between −1.81‰ and −5.92‰, and the δD values between −71.68‰ and −73.24‰, respectively. These isotopic data for kaolinite in altered granite-granodiorite complexes lie between meteoric water and primary magmatic H_2O, and thus reflect a meteoric/hydrothermal-alteration process at high temperature, similar to that described by Taylor (1974, 1979). The negative $\delta^{18}O$ and negative δD values of the kaolinite indicate hydrothermal alteration and depletion of ^2H and ^{18}O in which the prevailing temperatures led to large fractionation factors between liquid and vapor. The O-isotope value is explained by the fact that fractionation decreased due to an increase in temperature, which allowed the $\delta^{18}O$ value of the water

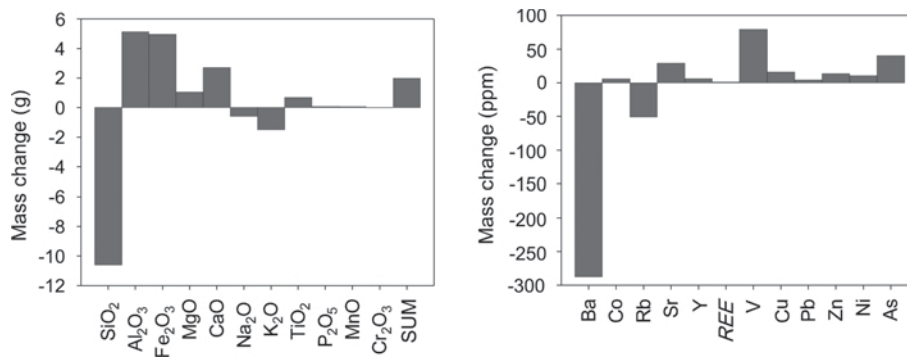

Figure 7. Changes in mass of major (g) and trace elements (ppm) in the study area.

Table 2. Major (wt.%) and trace-element (ppm) compositions of various lithologies of the study area (see Table 1 for mineralogical compositions of the samples).

Major oxides (wt.%)	Sedimentary units							
	C-2	C-8	D-14	F-9	K-2	K-8	K-10	Avg. sed.
SiO_2	61.06	49.42	52.90	54.21	64.84	55.12	40.91	54.07
Al_2O_3	19.64	24.48	21.49	28.27	20.26	20.69	12.23	21.01
Fe_2O_3*	4.89	7.38	3.70	1.14	2.03	8.15	10.53	5.40
MgO	1.08	3.31	2.25	0.66	0.78	1.35	6.22	2.24
CaO	0.27	0.31	0.68	0.16	0.15	0.35	8.75	1.52
Na_2O	0.16	0.30	1.55	0.14	0.14	0.56	0.12	0.42
K_2O	1.95	4.33	2.03	2.83	2.90	2.56	1.59	2.60
TiO_2	1.39	1.31	3.59	1.37	1.31	1.22	0.86	1.58
P_2O_5	0.06	0.19	0.28	0.04	0.05	0.08	0.11	0.12
MnO	0.03	0.07	0.02	0.01	0.01	0.02	0.09	0.04
Cr_2O_3	0.018	0.032	0.044	0.015	0.023	0.018	0.015	0.02
LOI	9.40	8.60	11.40	11.10	7.30	9.80	18.50	10.87
TOT/C	0.45	0.51	0.35	0.57	0.35	0.13	3.44	0.83
TOT/S	0.01	0.01	0.02	0.01	0.01	0.03	0.01	0.01
SUM	99.96	99.75	99.95	99.95	99.81	99.93	99.94	99.90
Ba	379.00	653.80	387.30	513.60	492.50	528.80	316.90	467.40
Be	4.00	5.00	2.00	10.00	4.00	3.00	3.00	4.43
Co	12.80	31.10	9.60	8.50	10.10	13.50	14.60	14.30
Cs	10.30	9.20	7.90	11.00	10.10	12.10	4.90	9.36
Ga	25.60	33.20	30.60	35.50	24.10	27.20	15.90	27.40
Hf	7.80	7.20	7.60	6.90	6.80	7.00	4.60	6.80
Nb	21.20	18.50	35.30	24.40	19.00	20.80	12.00	21.60
Rb	170.30	174.80	82.50	165.90	126.60	133.50	64.10	131.10
Sn	4.00	7.00	5.00	6.00	3.00	5.00	2.00	4.57
Sr	158.60	54.80	76.70	48.20	137.00	229.70	374.10	154.10
Ta	1.70	1.50	2.60	2.10	1.40	1.60	0.90	1.70
Th	25.20	21.10	9.00	17.40	12.20	24.20	7.30	16.60
U	2.90	5.40	2.90	8.40	2.70	3.80	5.00	4.40
V	183.00	214.00	308.00	140.00	138.00	163.00	139.00	183.60
W	4.40	4.30	4.40	4.80	3.50	3.40	2.50	3.90
Zr	276.90	241.50	279.00	241.40	251.10	239.90	155.50	240.80
Y	32.80	45.20	27.50	32.90	34.90	29.10	31.50	33.40
Sc	18.00	29.00	29.00	20.00	19.00	22.00	19.00	22.30
Mo	0.10	0.20	<0.10	0.10	<0.10	0.30	0.90	0.30
Cu	44.10	80.40	105.50	28.90	49.60	31.90	43.20	54.80
Pb	18.70	29.10	13.40	18.80	8.80	19.00	14.70	17.50
Zn	41.00	178.00	510.00	80.00	21.00	71.00	111.00	144.60
Ni	31.40	97.20	30.60	21.70	17.50	27.10	49.70	39.30
As	2.00	1.90	8.90	3.10	2.90	0.90	4.00	3.40
Cd	<0.10	0.20	0.20	0.40	<0.10	0.10	0.40	0.21
Sb	0.60	0.90	1.00	0.70	0.10	0.30	0.30	0.56
Bi	0.60	0.60	0.20	0.60	0.50	0.80	0.30	0.51
Au (ppb)	2.40	1.60	2.00	2.60	2.10	3.20	1.60	2.21
Hg	0.14	0.71	0.37	0.12	0.56	0.24	0.13	0.32
La	47.50	55.40	36.00	51.00	48.80	52.10	32.10	46.13
Ce	100.20	113.00	73.50	101.30	91.10	102.40	60.40	91.70
Pr	11.27	13.16	9.18	11.70	10.70	10.58	7.01	10.51
Nd	42.80	51.90	39.50	43.50	40.60	38.60	29.8	40.96
Sm	8.60	10.10	8.00	7.70	7.40	6.80	5.90	7.79
Eu	1.80	2.24	2.38	1.58	1.57	1.63	1.53	1.82
Gd	6.35	8.63	7.60	6.04	5.58	5.06	5.45	6.39
Tb	1.05	1.49	1.11	1.06	0.96	0.90	0.85	1.06
Dy	6.30	8.74	5.78	6.01	5.52	5.47	5.43	6.18
Ho	1.18	1.63	1.08	1.08	1.13	0.95	1.00	1.15
Er	3.31	4.58	3.00	3.09	3.46	3.05	3.04	3.36
Tm	0.54	0.63	0.43	0.50	0.57	0.48	0.45	0.51
Yb	3.22	4.30	2.52	3.09	3.17	2.96	2.51	3.11
Lu	0.54	0.64	0.47	0.44	0.53	0.50	0.42	0.51

Fe_2O_3*: total Fe oxides; LOI: loss on ignition

Table 2 (*contd.*)

Major oxides (wt.%)	Fresh granite to granodiorite											Altered granite to granodiorite						
	A-1	A-4	A-6	B-2	D-20	E-2	E-6	F-1	J-8	J-9	Avg. fresh	A-3	B-3	B-4	B-6	C-1	J-6	Avg. altered
SiO_2	74.42	73.18	72.93	72.88	85.84	70.19	69.27	74.31	74.88	74.22	74.21	58.58	62.51	49.47	63.43	52.37	62.81	58.20
Al_2O_3	12.83	16.03	16.37	14.48	6.82	16.24	18.55	15.75	14.79	15.58	14.74	16.47	18.13	14.98	21.39	15.20	21.17	17.89
Fe_2O_3*	2.87	0.45	0.61	1.42	1.38	2.54	1.00	0.73	0.36	0.39	1.18	7.92	6.17	6.50	2.19	8.88	0.72	5.40
MgO	0.15	0.19	0.22	0.26	0.34	0.37	0.71	0.32	0.17	0.13	0.29	0.63	0.23	2.77	0.28	2.51	0.67	1.18
CaO	0.41	0.11	0.08	1.30	0.41	0.50	0.13	0.07	0.39	0.11	0.35	2.40	0.66	7.79	0.72	3.83	0.71	2.69
Na_2O	3.70	1.94	1.37	3.13	0.07	2.65	1.68	0.15	1.30	0.51	1.65	1.18	0.67	1.95	1.27	0.14	0.71	0.99
K_2O	2.64	3.66	3.66	2.44	1.50	2.88	3.36	2.58	4.39	5.28	3.24	1.89	1.35	1.05	1.82	2.01	1.67	1.63
TiO_2	0.25	0.40	0.49	0.25	0.13	0.62	0.80	0.61	0.20	0.17	0.39	0.78	1.02	0.41	1.00	1.38	1.17	0.96
P_2O_5	0.05	0.01	0.01	0.04	0.03	0.08	0.03	0.03	0.23	0.09	0.06	0.11	0.17	0.06	0.17	0.10	0.14	0.13
MnO	0.04	0.01	0.01	0.03	0.01	0.04	0.01	0.01	0.01	0.01	0.02	0.02	0.09	0.11	0.02	0.11	0.06	0.07
Cr_2O_3	0.001	0.002	0.002	0.001	0.001	0.004	0.005	0.007	0.001	0.001	0.00	0.003	0.007	0.003	0.007	0.018	0.017	0.01
LOI	2.40	4.00	4.20	3.80	3.50	3.70	4.30	5.40	3.30	3.40	3.80	10.00	9.00	14.80	7.60	13.40	10.20	10.83
TOT/C	0.02	0.01	0.01	0.22	0.37	0.05	0.01	0.08	0.02	0.01	0.08	0.40	0.01	2.11	0.01	2.59	0.09	0.87
TOT/S	0.01	0.01	0.01	0.01	0.01	0.01	0.01	0.01	0.01	0.01	0.01	0.01	0.01	0.01	0.01	0.01	0.01	0.01
SUM	99.76	99.98	99.95	100.02	100.03	99.81	99.85	99.98	100.02	99.89	100.02	99.99	100.01	99.90	99.90	99.95	100.05	100.84
Ba	1188.80	787.10	710.50	307.00	292.60	579.60	411.40	533.80	327.10	298.70	543.70	357.00	285.90	128.20	223.90	340.80	169.40	250.87
Be	2.00	2.00	1.00	2.00	1.00	2.00	3.00	2.00	2.00	2.00	1.90	4.00	2.00	2.00	2.00	2.00	4.00	2.67
Co	4.10	0.60	3.10	3.40	2.40	18.90	7.00	3.40	0.50	0.60	4.40	5.50	9.10	14.20	8.90	18.10	3.40	9.87
Cs	1.30	2.30	2.30	3.20	0.80	3.00	5.00	4.20	3.20	4.90	3.00	5.70	7.90	9.10	6.10	5.50	3.40	6.28
Ga	13.90	17.00	17.500	15.30	7.20	17.10	20.30	18.60	18.60	19.30	16.50	20.80	20.60	13.60	22.60	20.30	28.40	21.05
Hf	3.00	4.00	4.50	3.10	4.40	5.90	4.80	5.40	2.30	2.10	4.00	4.50	3.50	2.10	2.80	6.40	2.90	3.70
Nb	5.30	7.50	8.30	8.20	3.30	9.10	8.10	10.50	11.00	13.40	8.50	9.90	7.70	6.30	7.90	17.20	8.10	9.52
Rb	61.70	116.50	122.10	81.20	33.80	112.00	171.80	100.80	168.90	236.40	120.50	78.10	47.60	38.60	77.70	100.60	67.20	68.30
Sn	<1.00	2.00	2.00	2.00	12.00	2.00	3.00	2.00	3.00	10.00	3.90	2.00	1.00	1.00	2.00	3.00	3.00	2.00
Sr	100.40	80.40	56.00	152.80	87.60	166.50	42.40	44.90	216.30	138.90	108.60	137.20	85.80	219.60	113.70	201.20	53.00	135.08
Ta	0.30	0.90	1.20	0.80	0.40	1.00	0.80	1.20	1.50	2.10	1.02	0.80	0.60	1.00	0.70	1.50	0.70	0.88
Th	4.50	13.60	11.40	16.10	4.80	15.90	9.00	12.60	8.30	5.30	10.20	5.20	3.70	10.90	4.70	12.10	3.70	6.72
U	2.10	2.10	2.30	1.60	5.40	2.20	2.10	5.10	7.90	3.60	3.50	3.20	1.80	4.10	2.40	2.10	1.70	2.55
V	17.00	68.00	76.00	49.00	20.00	108.00	145.00	67.00	12.00	9.00	57.10	120.00	161.0	92.0	118.00	147.00	165.00	133.83
W	2.30	1.100	1.30	1.40	4.00	1.50	1.90	2.10	0.80	2.90	1.90	12.10	2.80	1.00	9.20	3.70	2.10	5.15
Zr	135.50	118.40	128.60	83.10	124.50	188.10	150.70	197.90	62.50	59.70	124.90	136.20	135.00	56.90	87.20	219.40	100.10	122.47
Y	8.30	13.60	13.90	8.00	8.60	17.10	22.10	22.80	19.00	13.40	14.70	25.80	15.60	26.70	8.70	30.80	13.70	20.22
Sc	5.00	8.00	9.00	7.00	7.00	19.00	33.00	10.00	3.00	4.00	10.50	27.00	25.00	22.00	16.00	18.00	21.00	21.50
Mo	0.30	0.10	0.20	0.40	0.40	1.10	0.20	0.20	0.20	0.20	0.30	0.50	0.40	0.60	0.20	0.10	0.20	0.33
Cu	1.90	4.70	3.80	2.10	4.80	5.10	16.40	5.20	2.90	2.80	5.00	13.10	16.10	20.60	6.10	55.80	12.10	20.63
Pb	5.50	4.30	2.60	3.70	5.90	9.90	7.80	13.30	4.30	4.20	6.20	15.30	11.00	4.70	14.70	11.30	3.50	10.08
Zn	34.00	10.00	20.00	13.00	20.00	69.00	50.00	14.00	8.00	5.00	24.30	50.00	36.00	46.00	15.00	71.00	5.00	37.17
Ni	1.60	0.80	1.60	1.60	2.90	7.00	1.60	3.20	1.00	0.80	2.20	4.70	7.80	6.90	2.60	51.70	1.10	12.47
As	8.40	2.60	8.50	3.20	2.00	16.40	2.40	<0.50	1.60	<0.50	4.61	35.30	53.30	35.60	135.00	0.80	2.00	43.67

Cd	<0.10	<0.10	0.10	<0.10	<0.10	0.10	<0.10	<0.10	<0.10	<0.10	<0.10	<0.10	<0.10	<0.10	0.20	<0.10	0.10	<0.10	<0.10	<0.10	<0.10	<0.12
Sb	0.20	0.20	0.30	0.10	0.10	0.20	0.10	0.10	<0.10	0.20	1.10	0.90	0.10	0.10	0.10	0.90	0.50	0.50	<0.10	0.90	0.70	0.70
Bi	<0.10	0.10	1.10	<0.10	<0.10	0.80	<0.10	0.90	0.30	0.70	0.20	0.30	0.10	0.30	0.10	0.30	0.20	0.20	0.90	0.90	0.33	0.33
Au (ppb)	3.20	2.60	1.40	2.50	5.00	0.60	1.30	<0.50	1.00	1.90	1.60	0.50	1.70	<0.50	2.10	0.60	1.17					
Hg	0.01	0.01	0.02	<0.01	0.05	0.01	<0.01	0.01	0.01	0.02	0.03	<0.01	<0.01	<0.01	0.04	0.01	0.018					
La	17.60	16.00	16.40	9.80	6.90	30.20	28.10	34.20	21.40	18.89	27.20	18.20	16.60	16.30	33.80	12.40	20.75					
Ce	31.30	31.10	34.80	21.50	9.80	53.30	56.50	63.20	43.90	36.34	44.20	31.50	31.40	26.20	67.10	26.10	37.75					
Pr	3.09	3.54	3.88	2.12	1.33	5.52	6.77	6.99	5.13	4.05	5.17	4.08	3.79	3.19	8.38	3.13	4.62					
Nd	11.20	12.40	13.80	7.90	5.10	19.00	27.90	26.80	20.70	15.27	20.10	15.30	14.50	12.40	32.40	13.00	17.95					
Sm	1.80	2.10	2.60	1.60	1.00	3.80	5.10	4.80	4.70	2.97	4.00	2.90	3.20	2.20	6.90	2.40	3.60					
Eu	0.45	0.51	0.57	0.35	0.25	0.84	1.15	0.57	0.77	0.59	0.96	0.92	1.07	0.58	1.57	0.69	0.97					
Gd	1.55	2.31	2.42	1.35	1.02	3.39	4.33	3.87	4.29	2.67	3.57	3.09	3.36	1.72	5.64	2.26	3.27					
Tb	0.27	0.41	0.41	0.20	0.19	0.55	0.70	0.66	0.68	0.45	0.72	0.52	0.57	0.26	0.96	0.40	0.57					
Dy	1.52	2.40	2.57	1.28	1.18	3.14	3.88	3.55	3.53	2.53	4.21	2.91	3.99	1.80	5.73	2.25	3.48					
Ho	0.29	0.53	0.53	0.25	0.24	0.51	0.82	0.74	0.54	0.49	0.85	0.60	0.80	0.33	1.12	0.46	0.69					
Er	0.76	1.57	1.70	0.83	1.02	1.79	2.39	2.30	1.41	1.48	2.57	1.77	2.37	0.90	3.16	1.42	2.03					
Tm	0.11	0.23	0.28	0.12	0.16	0.29	0.36	0.36	0.19	0.14	0.22	0.40	0.38	0.13	0.45	0.23	0.31					
Yb	0.62	1.66	1.86	0.84	1.07	1.73	2.30	2.13	0.94	1.00	1.42	2.36	1.91	2.65	0.84	2.85	1.63	2.04				
Lu	0.14	0.27	0.31	0.15	0.15	0.27	0.40	0.34	0.12	0.12	0.23	0.42	0.27	0.37	0.12	0.44	0.25	0.31				

Table 3. Mass gains and losses (g and ppm) for samples of the Söğüt area (based on the average composition of 100 g of fresh rock and constant Zr).

	Calculated components	Mass gains and losses
Major oxides (g)		
SiO_2	66.59	−10.61
Al_2O_3	20.47	5.13
Fe_2O_3	6.17	4.95
MgO	1.35	1.05
CaO	3.07	2.71
Na_2O	1.13	−0.59
K_2O	1.87	−1.50
TiO_2	1.10	0.69
P_2O_5	0.14	0.08
MnO	0.08	0.06
Cr_2O_3	0.01	0.01
SUM		1.98
Trace elements (ppm)		
Ba	255.84	−287.82
Be	2.72	0.82
Co	10.06	5.66
Cs	6.41	3.39
Ga	21.47	4.99
Hf	3.77	−0.18
Nb	9.71	1.77
Rb	69.66	−50.86
Sn	2.04	−1.76
Sr	137.76	29.14
Ta	0.90	−0.12
Th	6.85	−3.30
U	2.60	−0.84
V	136.49	79.39
W	5.25	3.32
Zr	124.90	0.00
Y	20.62	5.94
Mo	0.34	0.01
Cu	21.04	16.07
Pb	10.28	4.13
Zn	37.90	13.60
Ni	12.71	10.50
As	44.53	40.02
Sb	0.70	0.57
Bi	0.34	−0.31
Rare earth elements (ppm)		
La	21.16	2.27
Ce	38.50	2.16
Pr	4.72	0.67
Nd	18.31	3.04
Sm	3.67	0.70
Eu	0.98	0.39
Gd	3.34	0.67
Tb	0.58	0.13
Dy	3.55	1.02
Ho	0.71	0.22
Er	2.07	0.59
Tm	0.32	0.10
Yb	2.08	0.67
Lu	0.32	0.09
Average *REE*	7.16	0.91

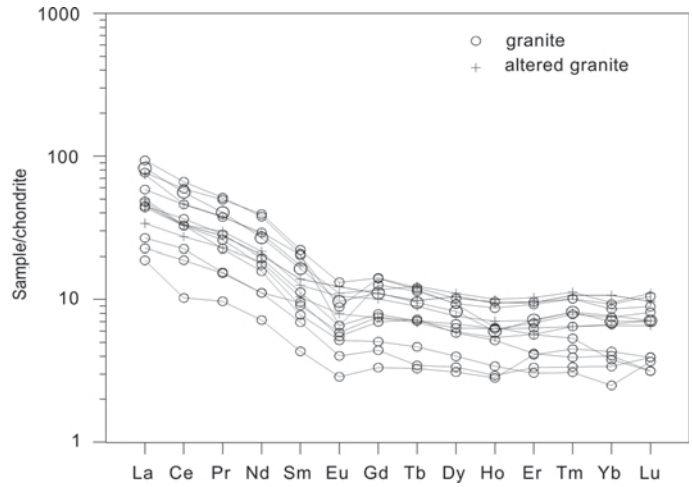

Figure 8. Chondrite-normalized *REE* patterns for Söğüt-area samples (Taylor and McLennan, 1985).

to more closely approach that of the rock at an elevated temperature than was possible at a low temperature. The flat horizontal and negative H values (consistent with only very minor variations), due to similar deuterium contents, may be attributed to smaller H contents of kaolinite as compared to water. This reveals that the hydrothermal water reacted, to varying degrees, with the granitic-granodioritic complexes and sedimentary units, exchanging some of its ^{16}O and ^{18}O from the source minerals of the rocks.

The mineralogic-petrographic data and the O-D isotopic compositions of the kaolinite fractions indicate that magmatic water was responsible for the formation of the kaolinite. Thus, the fluids for kaolinite formation can be considered to be of magmatic origin. Moreover, the isotopic relationships given in Figure 9 support this proposal. The $\delta^{18}O$ isotopic compositions of the magmatic water and granitic fluids are given by Taylor (1974, 1979) as 5.5 to +10%. If this component played an active role in the formation of the kaolinite, the formation temperature of kaolinite can be calculated easily using the equation of Anderson and Arthur (1983):

$$1000\ln\alpha(O)_{\text{kaolinite-fluid}} = +2.5(10^6/T^2) - 2.87$$
$$1000\ln\alpha(O)_{\text{kaolinite-water}} = \delta^{18}O_{\text{kaolinite}} - \delta^{18}O_{\text{fluid}}$$

where T is temperature (Kelvin).

Using this equation, the formation temperature of kaolinite was calculated (Table 5). Based on these results, the kaolinite studied may have formed between 164.54 and 477.23ºC. This temperature interval is consistent with high-temperature hydrothermal conditions.

DISCUSSION

The Paleozoic Sarıcakaya granitic-granodioritic complexes in the Soğüt area are cross-cut by aplitic and pegmatitic dikes, and are overlain by Neogene sedimentary units. Development of subvertical quartz veins, macro- and micro-fractures, and a network of cracks cross-cutting the kaolinite deposit in the granite-granodiorite reveals that kaolinization, silicification, and precipitation of Fe oxides were driven by injection of hydrothermal-fluid activities and processes (Nagasawa, 1978; Meunier, 1995; Boulais *et al.*, 2000; Meunier, 2005). Thus, kaolinite coexisting with illite developed along microfaults, veins, and fractures, apart from heterogenic occurrences of kaolinized feldspar, chloritized biotite, and hornblende and smectite coexisting with a widespread silicification and formation of Fe-oxide minerals.

An alternation of overlying Neogene fluvial and lacustrine conglomerate, sandstone, mudstone, and

Table 4. O- and H-isotopic compositions of kaolinite from the Söğüt area.

Sample	Standard deviation	$\delta^{18}O$ V-SMOW (‰)	Standard deviation	δD V-SMOW (‰)
A6	0.43	−1.81	0.83	−71.68
B3	0.52	−4.56	0.73	−73.84
E2	0.51	−5.92	0.14	−73.73

Table 5. The calculated formation temperature of the Söğüt-area kaolinites for magmatic waters having $\delta^{18}O$ compositions of 5.5‰ and 10‰ (Taylor, 1974, 1979).

$\delta^{18}O$ kaolinite (‰)	$\delta^{18}O$ fluid = 5.5‰	$\delta^{18}O$ fluid = 10‰
	T (ºC)	
−1.81	477.23	255.66
−4.56	316.52	189.30
−5.92	267.59	164.54

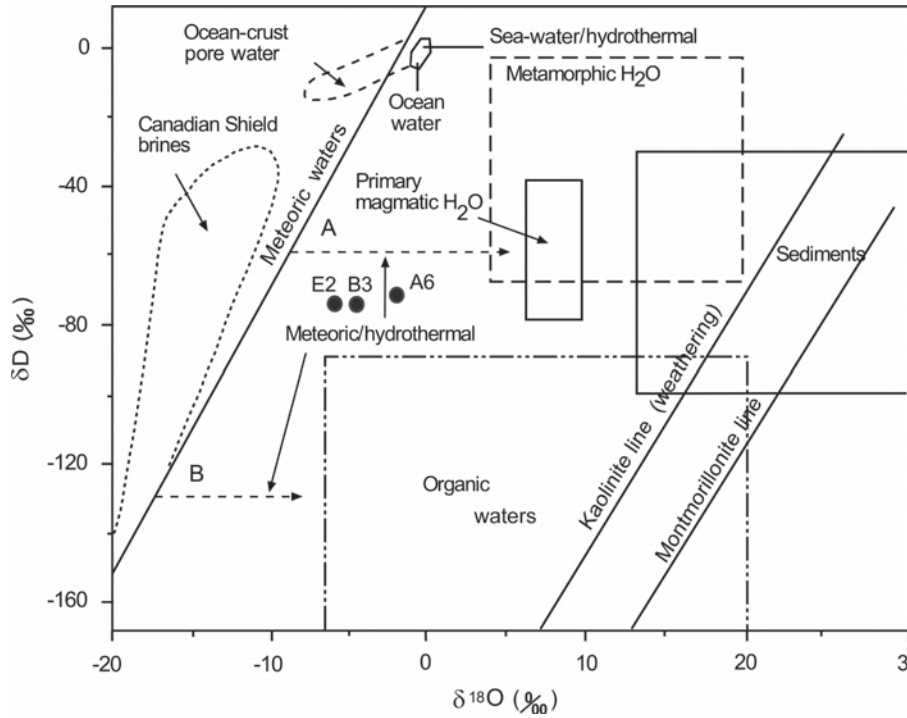

Figure 9. δD *vs.* $\delta^{18}O$ plots showing the isotopic compositions of the Söğüt-area kaolinites (A6, B3, and E2) (Sheppard, 1986). The line for kaolinite weathering is from Savin and Epstein (1970), and the line for smectite is from Sheppard and Gilg (1996) and Yui and Chang (1999).

claystone enclose thin coal lenses, root imprints, and leaf fossils and, locally, have conchoidal fracture and dessication cracks, revealing periodic climatic changes. These units are dominated by kaolinite, illite/biotite, and smaller amounts of smectite and, locally, chlorite coexisted with feldspar, quartz, and hornblende.

Textural images reveal that alteration of the granitic-granodioritic and sedimentary rocks is expressed through sericitization of feldspar and advanced kaolinization (increasing towards microfaults, veins, and fractures) in which hydrolysis and dissolution played important roles. Chen *et al.* (1997) and Parry *et al.* (1984) reported that feldspar is not altered directly to kaolinite but, rather, is first sericitized; kaolinization ensues with advancing alteration.

Micromorphologically, the association of feldspar crystals with kaolinite, the development of kaolinite plates parallel to microfractures and veins of granite-granodiorite, and the edging and rimming skeletal feldspar by book- or accordion-like kaolinite reveal that degradation of feldspar is due to hydrothermal-fluid flushing, resulting in the breakdown of feldspar in the parent rock, depletion of Na, Ca, and K, and significant gains in Al ± Fe which allowed for the development and precipitation of authigenic kaolinite under acidic environmental conditions (Nagasawa, 1978; Meunier, 1995; Inoue, 1995; Kadir and Karakaş, 2002; Kadir *et al.*, 2008). On the other hand, the dissolution of feldspar in the sedimentary units via flushing of meteoric and hydrothermal fluids through the open pore system of the sediments resulted in the dissolution of feldspar, release and gains of Al ± Fe, and leaching of alkali elements, thus favoring the precipitation of vermiform and irregular kaolinite under acidic environmental conditions.

The relatively low mobility of K in comparison to Na and Ca resulted in precipitation of authigenic illite in an alkaline environment (Aldaham and Morad, 1986; Ehrenberg, 1991; Berner and Berner, 1996; Ziegler, 2006). Chemical analyses give results that are consistent with the mineralogic compositions and the intensity of kaolinization. Thus, Al/Si ratios, Fe_2O_3+TiO_2, and LOI increased in the kaolinite-dominated material within the granitic-granodioritic rocks and overlying kaolinite-dominated sediments in comparison to the fresh granitic-granodioritic host rocks (Tables 1–2). Based on reflected-light microscopy determinations, the release of Fe (*e.g.* via dissolution of Fe-bearing biotite and hornblende) under reducing conditions – which favored the precipitation of Fe oxides (goethite, lepidocrocite) and Fe sulfide (pyrite) in veins and micro-fractures – also indicates flushing of acidic hydrothermal fluid in the environment, which resulted in local staining of the kaolinite deposit (*e.g.* Schwertmann and Murad, 1983; Schwertmann and Taylor, 1989; Eren and Kadir, 1999; Arslan *et al.*, 2006; Kadir and Akbulut, 2009). Similar environmental conditions also result in the precipitation of rutile due to the release of Ti during decomposition of biotite and hornblende, because Ti was replaced by Fe.

Furthermore, the coexistence of dark-gray manganite, mainly with goethite, as seen in reflected-light microscopy, was probably due to the presence of Mn in the hydrothermal fluid and microbial oxidation of Mn^{2+} (Robbins *et al.*, 1992; Leinemann *et al.*, 1997).

Depletion of Ba+Rb and related K and Na, along with a negative Eu anomaly, may be due to the alteration of K-feldspar (orthoclase-microcline) and plagioclase (albite-oligoclase) from the granite-granodiorite complex and overlying sedimentary units (Wilson, 1989; Rollinson, 1993). Also, enrichment of *LREE*s (such as La, Ce, and Nd; and Pr in the kaolinite-bearing sedimentary units) with increasing intensity of alteration in the granite-granodiorite complexes relative to the *HREE*s in the kaolinized materials may be attributed to the presence of garnet and hornblende in the source, although the effect of hornblende is not as great as that of garnet (Wilson, 1989; Rollinson, 1993). Moreover, fractionation may result from adsorption of the *LREE* onto authigenic crystals of kaolinite, illite, smectite, and chlorite, and from the coexistence of Fe phases, such as goethite, lepidocrocite, and pyrite, because of an increase in *LREE* with increasing alteration, or reflect decreasing mobility of *REE*s with increasing atomic weight of the stability constants of the elements in solution (Juteau *et al.*, 1978). Moreover, the negative $\delta^{18}O$ and negative δD values for the kaolinite fraction plot between meteoric and primary magmatic water, and the calculated formation temperature of the kaolinites from the Söğüt area also indicates that kaolinization of metastable plagioclase and K-feldspar in the granite-granodiorite-pegmatite-aplite complexes may have formed by hydrothermal processes.

In places, the association of kaolinite with smectite, and locally with chlorite, is controlled by the concentrations of Fe, Mg, and Al as well as the Na and Ca available in the environment, which were derived from the alteration of ferromagnesian minerals (*e.g.* biotite and hornblende) and plagioclase. Aldaham and Morad (1986) reported that K-feldspar is commonly replaced by illite and chlorite, and that chloritization occurs during release of Fe+Mg from alteration of biotite and hornblende. The association of chlorite with smectite may also indicate that chlorite formed at high temperature by conversion from smectite (Kristmannsdottir, 1978). Excess silica made available during the alteration process resulted in the precipitation of quartz along with some poorly crystalline phases (*e.g.* Meunier and Velde, 2004).

CONCLUSIONS

The presence of subvertical quartz veins, fractures, and veins bearing goethite, lepidocrocite, rutile, manganite, and pyrite, the occurrence of oxybiotite and oxyhornblende within the granite-granodiorite-pegmatite-aplite complex, local reddish staining of kaolinite deposits, increasing kaolinization and illitization toward veins and fractures, and outward to relatively heterogenic occurrences of sericitized-kaolinized feldspar, chloritized biotite and hornblende, and smectite, reveal that sericite, kaolinite, illite, chlorite, Fe-Ti-Mn oxide minerals, quartz, and poorly crystalline silica phases developed by flushing of hydrothermal acidic fluids through the paleoenvironement.

On the basis of edging of altered feldspar by vermiform and irregular, plate-like, stacked forms of kaolinite, depletion of Ba + Rb, and a negative Eu anomaly, the suggestion is that kaolinite was precipitated authigenically by dissolution of K-feldspar and plagioclase. Also, development of kaolinite plates parallel to microfracture axes, depletion of both $\delta^{18}O$ and δD, and the calculated formation temperature of kaolinite reveal that kaolinization, illitization, and silicification in the granite-granodiorite complex units developed under acidic physicochemical environmental conditions controlled by injection of hydrothermal fluids through microfaults, veins, and fractures that increased (Al+Fe)/Si and led to moderate depletion of K and leaching of mobile elements Ca and Na. Similar physicochemical environmental conditions were produced by hydrothermal fluids (with meteoric-water involvement) flushed through an open-pore system of sediments resulting in the authigenic precipitation of kaolinite in the overlying sedimentary units *via* a feldspar dissolution-kaolinite precipitation mechanism under acidic environmental conditions.

A combination of field observations and mineralogical, petrographic, and geochemical determinations clearly indicates that the kaolinite of the Söğüt area formed by hydrothermal-alteration processes that acted on rocks of the Paleozoic granite-granodiorite-pegmatite-aplite complex, and that alteration was driven by meteoric fluids and hydrothermal processes in the related overlying sedimentary units.

ACKNOWLEDGMENTS

This research includes further work on the second author's MSc study, which was supervised by the first author. The authors are indebted to anonymous reviewers for their extremely careful and constructive reviews, which significantly improved the quality of the paper. They are also grateful to Professor Warren Huff (University of Cincinnati, USA) and Professor Joseph W. Stucki (University of Illinois) for their insightful editorial comments and suggestions and to Dr Emel Abdioğlu (Karadeniz Technical University, Turkey) who helped with preparation of the geochemical figures. The authors thank the General Directorate of Mineral Research and Exploration of Turkey (MTA) for support in the conduct of some of the mineralogical analyses.

REFERENCES

Akıncı, Ö. (1968) Bilecik bölgesi kaolin yatakları ve civarının jeolojisi, kaolinlerin seramik özellikleri. *Maden Tetkik ve*

Arama Enstitüsü Dergisi, **70**, 67–82.

Aksoy, H. (1978) Geology and clay deposits of the Küreköy-Inhisar (Söğüt-Bilecik). Yüksek Mühendislik Tezi, O.D.T.Ü. Fen Bilimleri Enstitüsü, Ankara, 65 pp. (Unpublished MSc thesis).

Aldaham, A.A. and Morad, S. (1986) Mineralogy and chemistry of diagenetic clay minerals in Proterozoic sandstones from Sweden. *American Journal of Science*, **286**, 29–80.

Anderson, T.F. and Arthur, M.A. (1983) Stable isotopes of oxygen and carbon and their application to sedimentologic and paleoenvironmental problems. Pp. 1–151 in: *Stable Isotopes in Sedimentary Geology* (M.A. Arthur, T.F. Anderson, I.R. Kaplan, J. Veizer, and L.S. Land, editors). Short Course Notes, **10**, Society of Economic Paleontologists and Mineralogists.

Arslan, M., Kadir, S., Abdioğlu, E., and Kolaylı, H. (2006) Origin and formation of kaolin minerals in saprolite of Tertiary alkaline volcanic rocks, Eastern Pontides, NE Turkey. *Clay Minerals*, **41**, 599–619.

Berner, E.K. and Berner, R.A. (1996) *Global Environment: Water, Air, and Geochemical Cycles*. Prentice-Hall, New Jersey, USA, 376 pp.

Bobos, I., Duplay, J., Rocha, J., and Gomes, C. (2001) Kaolinite to halloysite-7 Å transformation in the kaolin deposit of São vicente de Pereira, Portugal. *Clays and Clay Minerals*, **49**, 596–607.

Boulais, P., Valley, J.M., Choux, J.E., Fourcade, S., and Martineau, F. (2000) Origin of kaolinization in Brittany (NW France) with emphasis on deposits over granite: stable isotopes (O, H) constraints. *Chemical Geology*, **168**, 211–223.

Brindley, G.W. (1980) Quantitative X-ray analysis of clays. Pp. 411–438 in: *Crystal Structures of Clay Minerals and their X-ray Identification* (G.W. Brindley and G. Brown, editors). Monograph **5**, Mineralogical Society, London.

Bristow, C.M. (1977) A review of the evidence for the origin of the kaolin deposits in S.W. England. *Proceedings of the 8th International Kaolin Symposium and Meeting on Alunite*, Madrid-Rome, K-2, 1–19.

Chen, P.Y., Lin, M.L., and Zheng, Z. (1997) On the origin of the name kaolin and the kaolin deposits of the Kauling and Dazhou areas, Kiangsi, China. *Applied Clay Science*, **12**, 1–25.

Çoğulu, E., Delaloye, E., and Chessex, R. (1965) Sur l'age de quelques rockes intrusives acides de la region Eskişehir, Turquie. *Archives des Sciences Genève*, **18**, 692–699.

Delaloye, M. and Bingöl, E. (2000) Granitoids from western and northwestern Anatolia: Geochemistry and modeling of Geodynamic Evolution. *International Geology Review*, **42**, 241–263.

Demirkol, C. (1977) Üzümlü-Tuzaklı (Bilecik ili) dolayının jeolojisi. *Tatbiki Jeoloji Kürsüsü Arşivi*, **20**, 9–16.

Duru, M., Gedik, İ. and Aksay, A. (2002) 1:100.000 ölçekli Türkiye Jeoloji Haritası. No. 37. The General Directorate of Mineral Research, Ankara.

Ehrenberg, S.N. (1991) Kaolinized, potassium-leached zones at the contacts of the Garn Formation, Haltenbanken, mid-Norwegian continental shelf. *Marine and Petroleum Geology*, **8**, 250–269.

Ekosse, G. (2001) Provenance of the Kgwakgwe kaolin deposit in southeastern Bostwana and its possible utilization. *Applied Clay Science*, **20**, 137–152.

Eren, M. and Kadir, S. (1999) Colour origin of upper Cretaceous pelagic red sediments within the Eastern Pontides, northeast Turkey. *International Journal of Earth Sciences*, **88**, 593–595.

Exley, C.S. (1976) Observations on the formation of kaolinite in the St. Austell Granite, Cornwall. *Clay Minerals*, **11**, 51–63.

Farmer, V.C. and Palmieri, F. (1975) The characterization of soil minerals by infrared spectroscopy. Pp. 573–671 in: *Soil Components, vol. 2, Inorganic Components* (J.E. Gieseking, editor). Springer-Verlag, New York.

Garbarino, C., Masi, U., Padalino, G., and Palomba, M. (1994) Geochemical features of the kaolin deposits from the Sardinia (Italy) and genetic implications. *Chemie der Erde*, **54**, 213–233.

Gençoğlu, H. (1988) Yeniköy-Küre-Çaltı (Bilecik Söğüt) yöresi Neojen baseninin sedimanter jeolojik ve mineralojik-petrografik incelenmesi. Yüksek Mühendilik Tezi, Hacettepe Üniversitesi, Ankara, 147 pp. (unpublished MSc thesis).

Gençoğlu, H., Bayhan, H., and Yalçın, H. (1989) Bilecik-Söğüt Yöresi kaolinit yataklarının mineralojisi ve kökeni, IV. Ulusal Kil Sempozyumu. *C.Ü., Sivas*, 97–110.

Gilkes, R.J. and Suddhiprakarn, A. (1979a) Biotite alteration in deeply weathered granite. I. Morphological, mineralogical, and chemical properties. *Clays and Clay Minerals*, **27**, 349–360.

Gilkes, R.J. and Suddhiprakarn, A. (1979b) Biotite alteration in deeply weathered granite. II. The oriented growth of secondary minerals. *Clays and Clay Minerals*, **27**, 361–367.

Göncüoğlu, M.C., Turhan, N., Şentürk, K., Uysal, Ş., Özcan, A., and Işık, A. (1996) Orta Sakarya'da Nallıhan-Sarıcakaya arasındaki yapısal jeolojik özellikleri. MTA Report No. (Unpublished).

Göncüoğlu, M.C., Turhan, N., Şentürk, K., Özcan, A., Uysal, Ş., and Yılmaz, M. (2000) A geotraverse across northwestern Turkey: tectonic units of central Sakarya region and their tectonic evolution. Pp. 139–161 in: *Tectonics and Magmatism in Turkey and Surrounding Area* (E. Bozkurt, J.A. Winchester, and J.D.A. Piper, editors). Special Publications, **173**, Geological Society, London.

Gouveia, M.A., Prudencio, M.L., Figueiredo, M.O., Pereira, L.C.J., Waerenbrogh, J.C., Morgado, I., Pena, T., and Lopes, A. (1993) Behavior of REE and other trace and major elements during weathering of granitic rocks, Evora, Portugal. *Chemical Geology*, **107**, 293–298.

Gürel, A. and Kadir, S. (2008) Geology and mineralogy of Late Miocene clayey sediments in the southeastern part of the central Anatolian volcanic province, Turkey. *Clays and Clay Minerals*, **56**, 307–321.

Harris, W.G., Zelazny, L.W., Baker, J.C., and Martens, D.C. (1985a) Biotite kaolinization in Virginia Piedmont soils: I. Extent, profile trends, and grain morphological effects. *Soil Science Society of America Journal*, **49**, 1290–1297.

Harris, W.G., Zelazny, L.W., and Bloss, F.D. (1985b) Biotite kaolinization in Virginia Piedmont soils: II. Zonation in single grains. *Soil Science Society of America Journal*, **50**, 810–819.

Inoue, A. (1995) Formation of clay minerals in hydrothermal environments. Pp. 268–329 in: *Origin and Mineralogy of Clays: Clays and the Environment* (B. Velde, editor). Springer-Verlag, Berlin.

Juteau, T., Bingöl, F., Noack, Y., and Whitechurch, H. (1978) 38. Preliminary results: mineralogy and geochemistry of alteration products in leg 45 basement samples. *Initial Reports of the Deep Sea Drilling Project*, **XLV**, 613–645, Washington.

Kadir, S. and Akbulut, A. (2009) Mineralogy, geochemistry and genesis of the Taşoluk kaolinite deposits in pre-Early Cambrian metamorphites and Neogene volcanites of Afyonkarahisar, Turkey. *Clay Minerals*, **44**, 89–112.

Kadir, S. and Karakaş, Z. (2002) Mineralogy, chemistry and origin of halloysite, kaolinite and smectite from Miocene ignimbrites, Konya, Turkey. *Neues Jahrbuch für Mineralogie, Abhandlungen*, **177**, 113–132.

Kadir, S., Önen-Hall, P., Aydin, S.N., Yakicier, C., Akarsu, N., and Tuncer, M. (2008) Environmental effect and genetic influence: a regional cancer predisposition survey in the Zonguldak region of northwest Turkey. *Environmental Geology*, **54**, 391–409.

Kalyoncuoğlu, A., Özkan, Ü. and Aktaran, İ. (1977) Çatlı-Küre-Yeniköy (Bilecik-Söğüt) dolaylarının refrakter kil ve kaolen aramaları ara raporu. MTA Rapor No. 1310, 85 pp. (unpublished).

Kibici, Y. (1982) Sarıcakaya (Eskişehir ili) masifinin jeolojisi, petrografisi ve petrolojik etüdü, masife ilişkin kalay araştırması. Eskişehir Devlet Mühendislik ve Mimarlık Akademisi, Doktora Tezi, 224 pp.

Kitagawa, R. and Köster, H.M. (1991) Genesis of the Tirschenreuth kaolin deposit in Germany compared with the Kohdachi kaolin deposit in Japan. *Clay Minerals*, **26**, 61–79.

Kristmannsdottir, H. (1978) Alteration of basaltic rocks by hydrothermal activity at 100–300ºC. *Proccedings of International Clay Conference, Oxford*, pp. 359–367.

Leinemann, C.P., Taillefert, M., Perret, D., and Gaillard, J.F. (1997) Association of cobalt and manganese in aquatic systems: chemical and microscpic evidence. *Geochimica et Cosmochimica Acta*, **61**, 1437–1466.

MacEwan, D.M.C. and Wilson, M.J. (1980) Interlayer and intercalation complexes of clay minerals. Chapter 3 in: *Crystal Structures of Clay Minerals and their X-ray Identification* (G.W. Brindley and G. Brown, editors). Monograph **5**, Mineralogical Society, London.

Maclean, W.H. and Kranidiotis, P. (1987) Immobile elements as monitors of mass transfer in hydrothermal alteration: Phelps Dodge massive sulfide deposits, Matagami, Quebec. *Economic Geology* **2**, 951–962.

Madejová, P., Komadel, P., and Čičel, B. (1992) Infrared spectra of some Czech and Slovak smectites and their correlation with structural formulas. *Geologica Carpathica Clays*, **1**, 9–12.

Maiza, P.J., Pieroni, D., and Marfil, S.A. (2003) Geochemistry of hydrothermal kaolins in the SE area of Los Menucos, Province of Rio Negro, Argentina. Pp. 123–130 in: *A Clay Odyssey* (E.A. Dominguez, G.R. Mas and F. Gravero, editors). Elsevier, Amsterdam.

Meunier, A. (1995) Hydrothermal alteration by veins. Pp. 247–267 in: *Origin and Mineralogy of Clays, Clays and the Environment* (B. Velde, editor). Springer-Verlag Berlin.

Meunier, A. (2005) *Clays*. Springer-Verlag, Berlin, Heidleberg, Germany, 472 pp.

Meunier, A. and Velde, B. (2004) *Illite, Origin, Evolution and Metamorphism*. Springer-Verlag, Berlin, Heidelberg, New York, 286 pp.

Moore, D.M. and Reynolds, R.C. (1989) *X-ray Diffraction and the Identification and Analysis of Clay Minerals*. Oxford University Press, New York, 332 pp.

Nagasawa, K. (1978) Kaolin minerals. Pp. 189–219 in: *Clays and Clay Minerals of Japan* (T. Sudo and S. Shimoda, editors). Developments in Sedimentology, **26**, Elsevier, Tokyo.

Njoya, A., Nkoumbou, C., Grosbois, C., Njopwouo, D., Njoya, D., Courtin-Nomade, A., Yvon, J., and Martin, F. (2006) Genesis of Mayouom kaolin deposit (western Cameroon). *Applied Clay Science*, **32**, 125–140.

Parry, W.T., Ballantyne, J.M., and Jacobs, D.C. (1984) Geochemistry of hydrothermal sericite from Roosevelt Hot Springs and the Tintic and Santa Rita porphyry copper systems. *Economic Geology*, 79, 72–86.

Rebertus, R.A., Weed, S.B., and Buol, S.W. (1986) Transformations of biotite to kaolinite during saprolite-soil weathering. *Soil Science Society of America Journal*, **50**, 810–819.

Robbins, E.I., Agostino, J.P.D., Ostwald, J., Fanning, D.S., Carter, V., and Van Hoven, R.L. (1992) Manganese nodules and microbial oxidation of manganese in the Huntley Meadows Wetland, Virginia, USA. *Catena Supplement*, **21**, 179–202.

Rollinson, H.R. (1993) *Using Geochemical Data: Evaluation, Presentation, Interpretation*. John Wiley and Sons Inc., New York, 352 pp.

Russell, J.D. (1987) Infrared methods. Pp. 133–173 in: *A Handbook of Determinative Methods in Clay Minerals* (M.J. Wilson, editor). Blackie, Glasgow, UK.

Savin, S.M. and Epstein, S. (1970) The oxygen and hydrogen isotope geochemistry of clay minerals. *Geochimica et Cosmochimica Acta*, **34**, 25–42.

Schwertmann, U. and Murad, E. (1983) Effect of pH on the formation of goethite and hematite from ferrihydrite. *Clays and Clay Minerals*, **31**, 277–284.

Schwertmann, U. and Taylor, R.M. (1989) Iron oxides. Pp. 379–438 in: *Minerals in Soil Environments* (J.B. Dixon and S.B. Weed, editors). Soil Science Society of America, Madison, Wisconsin, USA.

Şengör, A.M.C. (1979) The North Anatolian Transform Fault: its age, offset and tectonic significance. *Journal of the Geological Society*, **13**, 268–282.

Şengör, A.M.C. and Yılmaz, Y. (1981) Tethyan evolution of Turkey: a plate tectonic approach. *Tectonophysics*, **75**, 181–241.

Sheppard, S.M.F. (1986) Characterization and Isotopic Variations in Natural Waters. Pp. 141–162 in: Stable Isotopes in High Temperature Geological Processes (J.W. Valley, H.P. Taylor, and J.R. O'Neil, editors). Reviews in Mineralogy, **16**, Mineralogical Society of America, Washington, D.C.

Sheppard, S.M.F. and Gilg, H.A. (1996) Stable isotope geochemisty of clay minerals. *Clay Minerals*, **31**, 1–24.

Siddique, M.A. and Ahmed, Z. (2008) Geochemistry of the kaolin deposits of Swat (Pakistan). *Chemie der Eder Geochemistry*, **68**, 207–219.

Srasra, E., Bergaya, F., and Fripiat, J.J. (1994) Infrared spectroscopy study of tetrahedral and octahedral substitutions in an interstratified illite-smectite clay. *Clays and Clay Minerals*, **42**, 237–241.

State Planning Organization of Turkey (2001) State Planning Organization of Turkey, 8th Five-Year Development Plan, Mining Special Expert Commission Report, Volume 1, Industrial Minerals Sub-Commission, Ceramic clays–Kaolin–Pyrophyllite–Wollastonite–Talc Group, Ankara, 224 pp. (http://ekutup.dpt.gov.tr/madencil/sanayi-ha/oik618.pdf)

Stock, L. and Sikora, W. (1976) Transformation of micas in the process of kaolinization of granites and gneisses. *Clays and Clay Minerals*, **24**, 156–162.

Taylor, H.P. (1974) The application of oxygen and hydrogen isotope studies to problems of hydrothermal alteration and ore deposition. *Economic Geology*, **69**, 843–883.

Taylor, H.P. (1979) Oxygen and hydrogen relationships in hydrothermal mineral deposits. Pp. 236–277 in: *Geochemistry of Hydrothermal Ore Deposits* (H.L. Barnes, editor) 2nd edition. Wiley, New York.

Taylor, S.R. and McLennan, S.M. (1985) *The Continental Crust: Its Composition and Evolution*. Blackwell, Oxford, 312 pp.

Van der Marel, H.W. and Beutelspacher, H. (1976) *Atlas of IR Spectroscopy of Clay Minerals and Their Admixtures*. Elsevier, Amsterdam, 396 pp.

Wilson, M.J. (1987) X-ray powder diffraction methods. Pp. 26–98 in: *A Handbook of Determinative Methods in Clay Mineralogy* (M.J. Wilson, editor). Blackie, Glasgow, UK.

Yui, T.F. and Chang, S.S. (1999) Formation conditions of

vesicle/fissure-filling smectites in Penghu basalts: a stabe-isotope assessment. *Clay Minerals*, **34**, 381–393.

Ziegler, K. (2006) Clay minerals of the Permian Rotliegend Group in the North Sea and adjacent areas. *Clay Minerals*, **41**, 355–393.

Zielinski, R.A. (1985) Element mobility during alteration of silicic ash to kaolinite - a study of tonstein. *Sedimentology*, **32**, 567–579.

(*Received 11 February 2008; revised 28 January 2009; Ms. 122; A.E. W. Huff*)